


**The University of Jordan
Authorization Form**

I, Khalifa Isa Burshied , authorize the University of Jordan to supply copies of my Thesis/ Dissertation to libraries or establishments or individuals on request, according to the University of Jordan regulations.

Signature: 

Date: 20 / 11 / 2010

نموذج رقم (١٨)
اقرار والتزام بقوانين الجامعة الأردنية وأنظمتها
وتعليماتها لطلبة الماجستير والدكتوراة

أنا الطالب: خلينة سعيد بيبي الرقم الجامعي: ٨٠٧١٦٨٤
التخصص: ميتا نيد الكلية: الدراسات العليا

عنوان الرسالة / الاطروحة

The reduction of soot formation from fuels using
Oxygenates additives

أعلن بأنني قد التزمت بقوانين الجامعة الأردنية وأنظمتها وتعليماتها وقراراتها السارية المفعول المتعلقة باعداد رسائل الماجستير والدكتوراة عندما قمت شخصيا" باعداد رسالتي / اطروحتي ، وذلك بما ينسجم مع الأمانة العلمية المتعارف عليها في كتابة الرسائل والأطاريح العلمية. كما أنني أعلن بأن رسالتي /اطروحتي هذه غير منقولة أو مستلة من رسائل أو أطاريح أو كتب أو أبحاث أو أي منشورات علمية تم نشرها أو تخزينها في أي وسيلة اعلامية، وتأسيسا" على ما تقدم فإنني أتحمّل المسؤولية بأنواعها كافة فيما لو تبين غير ذلك بما فيه حق مجلس العمداء في الجامعة الأردنية بالغاء قرار منحي الدرجة العلمية التي حصلت عليها وسحب شهادة التخرج مني بعد صدورها دون أن يكون لي أي حق في التظلم أو الاعتراض أو الطعن بأي صورة كانت في القرار الصادر عن مجلس العمداء بهذا الصدد.

التاريخ: ١٨ / ١١ / ٢٠١٠

توقيع الطالب: خلينة سعيد بيبي

تعتمد كلية الدراسات العليا
هذه النسخة من الرسالة
التوقيع: خلينة سعيد بيبي التاريخ: ١٨ / ١١ / ٢٠١٠

**THE REDUCTION OF SOOT FORMATION FROM FUELS USING
OXYGENATES ADDITIVES**

By
Khalifa Isa Burshaied

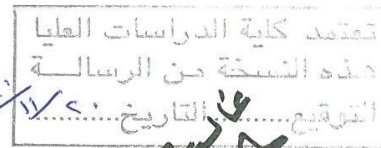
Supervisor
Dr. Mohammad A. Hamdan , Prof.

**This Thesis was Submitted in Partial Fulfillment of the Requirements for the Master's
Degree of Science in Mechanical Engineering**

Faculty of Graduate Studies

The University of Jordan

Nov, 2010



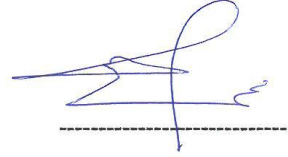
COMMITTEE DECISION

This Thesis/Dissertation (The reduction of soot formation from fuels using oxygenates additives) was successfully Defended and Approved on 11/11/2010

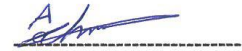
Examination Committee

Signature

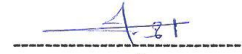
Dr. Mohammad A. Hamdan , (Supervisor)
Prof. of Mechanical Engineering



Dr. Ahmed AL-Salaymeh , (Member)
Assoc. Prof. of Mechanical Engineering



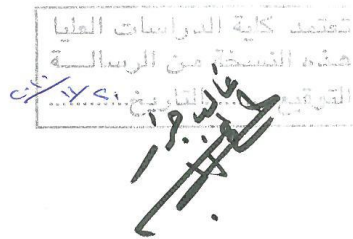
Dr. Ahmad Sakhrieh, (Member)
Assist. Prof. of Mechanical Engineering



Dr. Mahmood Z. Abu-Zaid (Member)
Prof. of Mechanical Engineering
Mutah University



تعتمد كلية الدراسات العليا
هذه النسخة من الرسالة
التاريخ 11/11/2010



DEDICATION

This work is dedicated to

My father, my mother, my wife, my sisters and my brothers

ACKNOWLEDGMENT

Many people helped me during my work, firstly; I would like to state my thanks to my supervisor Prof. Dr. Mohammad A. Hamdan for his continuous support and guidance.

Many thanks to Mr. Aref Shaheen for his support through technical consultations. I must not forget to mention my deep appreciation and thanks to Bahrain defense force for sending me to finish my study and still support me through my education.

TABLE OF CONTENTS

Subject	Page
Committee decision	li
Dedication	lii
Acknowledgement	Iv
Table of contents.....	V
List of tables	vii
List of figures.....	viii
Nomenclatures	Ix
List of Appendices	X
Abstract	Xi
Chapter one: Introduction	1
1.1 General.....	1
1.2 Objective.....	2
1.3 Layout of thesis.....	2
Chapter two: Literature review.....	3
Chapter three: Theoretical Background.....	8
3.1 Background.....	8
3.2 Soot visual detection	9
3.3 Temperature measurement principle.....	10
3.4 Pressure measurement principle.....	11
3.5 Fuel preparation	12
Chapter four: Testing facility and measurements	14
4.1 Selection of shock tube material.....	14
4.2 Shock tube	17
4.3 Electric heating pipe.....	21
4.4 Measuring device and measurement	23
Chapter five: Experimental procedure.....	26
Chapter Six: Experimental results.....	28
Chapter Seven: Conclusion and final remarks	34

References.....	35
Appendices	36
Abstract (in Arabic).....	42

LIST OF TABLES

Number	Table caption	Page
Table 5.1	Samples matrix	26
Table 6.1	Soot comparison matrix based on colour detection	33

LIST OF FIGURES

Number	Figure caption	Page
Figure(3.1)	Inner grade of the filter used	9
Figure(3.2)	Customized filter	10
Figure(3.3)	Thermocouple in drive section	11
Figure(3.4)	Pressure sensor	12
Figure (4.1)	Sketch of shock tubes	14
Figure (4.2)	Shock tube sketch	17
Figure (4.3)	Closed end in the drive section	18
Figure (4.4)	Flange coupling	19
Figure (4.5)	Shock tube membrane	20
Figure (4.6)	Electric heater coil installation around shock tube	21
Figure (4.7)	Heated shock tube	22
Figure (4.8)	Digital thermometer	23
Figure (4.9)	Pressure sensor setup	24
Figure (4.10)	Pressure sensor	25
Figure(5.1)	Filter placement at the tip of driven section	27
Figure (6.1)	Sample 1(A:Diesel),sample 5(B:Biofuel),sample 9(C:Emulsified)	28
Figure (6.2)	Sample 6 Biofuel with methanol	29
Figure (6.3)	Sample 2(A:Diesel),sample 6(B:Biofuel),sample 10(C:Emulsified)	29
Figure (6.4)	Sample 3(A:Diesel),sample 7(B:Biofuel),sample 11(C:Emulsified)	30
Figure (6.5)	Sample 12 (A: Emulsified fuel) vs. sample 8 (B: Biofuel)	31
Figure (6.6)	Sample 12 (A: Emulsified fuel) vs. sample 8 (B: Biofuel)	31
Figure (6.7)	Sample 12 Emulsified fuel mixed with acetone	32
Figure (6.8)	Sample 4 Diesel with acetone mixture	32
Figure (6.9)	Comparison between all samples based on (1-12) scale	33

NOMENCLATURE:

A	Area (m ²)
d	Diameter (m)
D	Pipe diameter (m)
E	Joint efficiency
H	Height (m)
k	Thermal conductivity (W/m.K)
L	Length (m)
m	Mass (kg)
\dot{m}	Mass flow rate (kg/s)
P	Pressure (Pa)
R _{pipe}	Pipe radius (m)
S	Material allowable strength (MPa)
t	Minimum allowable thickness (mm)
ρ	Density (kg/m ³)

LIST OF APPENDICES

Appendix	Caption	Page
Appendix (A)	Ratings for group 2.2 materials	36
Appendix (B)	List of material specifications	37
Appendix (C)	List of bolting specifications	38
Appendix (D)	Ratings for group 2.1 materials	39
Appendix (E)	Curve fit coefficient for fuel specific heat	40
Appendix (F)	Selection the material of high maximum allowable stress	41

THE REDUCTION OF SOOT FORMATION FROM FUELS USING OXYGENATES ADDITIVES

By
Khalifa Isa Burshaid

Supervisor
Dr. Mohammad A. Hamdan, Prof.

ABSTRACT

This work presents an experimental technique for the determination of soot formation in pure fuel, biofuel and emulsified fuel. That constitute this fuels was studied in a heated shock tube and investigated the possibility of reducing soot production in locally refined diesel, locally produced biofuel and emulsified fuel. This reduction was conducted using certain oxygenated additives. The pressure ranges 7 to 8.5 bars and temperature range was within 280 to 300 °C .

The results give a good indication of the effect for oxygenated additives in reducing the soot formation. It was found that methanol has maximum effect on soot reduction followed by ethanol and finally acetone.

CHAPTER ONE: INTRODUCTION

1.1 General:

It is known that soot “particulate matter” is a name given to the mixture of solid particles and liquid droplets found in air, the main constituents of this mixture is carbon. Soot is produced from many sources such as burning coal, diesel, wood etc.,. Cutting its emissions has a virtually instantaneous effect, because it rapidly falls out of the atmosphere, unlike carbon dioxide which remains there for over a hundred years. And because soot is one of the worst killers among all pollutants, radical reductions save lives and so should command popular and political support

This work investigates the possibility of reducing soot production from burning locally refined diesel, locally produced biofuel and emulsified fuel. This will be accomplished by the design, construction and testing of an experimental rig, which consists mainly of a shock tube, within which the combustible mixture is introduced and ignited and introduced to a customized filter. This filter is used to measure the concentration of soot that is produced during the burning of the fuel.

Further, this investigation of soot reduction had been conducted using certain oxygenated additives, these additives contain sufficient amount of oxygen, which enhances the burning of carbon (soot) and hence soot reduction increases. This research work aimed to reduce that soot, which contributes significantly to environmental problem in Jordan and hence cleaner environment. The alternative fuels such as biofuels and emulsified fuels are of high competitive to diesel fuel, this will reduce the national energy bill.

1.2 Objective:

This work presents an experimental technique for the determination of the soot formation in different fuels; diesel, biofuel and emulsified fuel that accomplish the main target for the reduction of soot formation by using oxygenated additives like methanol, ethanol and acetone. This will give a realistic way of how researchers can accomplish soot reduction for different fuels using oxygenated additives.

1.3 Layout of thesis:

This chapter is the first chapter, which introduces the reader to the subject. In chapter two, work conducted internationally is mentioned in order to clarify the connecting points between this work and others work, also to make use of similar works that has been done. Theoretical background in chapter three comes before the measurement work. This theory gives the principle of the proposed system configuration which will deliver the required results.

The testing facility has been extensively explained in chapter four for the purpose of giving guidance for any future work to be done and to explain the principle for each measuring instrument. The experimental procedure of this work will be explained in chapter five to show the reader the experimental work steps. The results were introduced in chapter six. Finally, the conclusion of this thesis has been mentioned in chapter seven to give a final decision about this experimental work and to verify the expected findings.

CHAPTER TWO: LITERATURE REVIEW

Mathieu et. al. (2009) studied the soot tendency (soot induction delay time and soot yield) of a diesel fuel surrogate and of the hydrocarbons that constitute this mixture was studied in a heated shock tube. The surrogate is composed of three hydrocarbons representative of major chemical families of diesel fuels (39% n-propylcyclohexane, 28% n-butylbenzene, and 33% 2,2,4,4,6,8,8-heptamethylnonane in mass proportion). Experiments were carried out for highly diluted mixtures in argon; in the case of pyrolysis and at two equivalence ratios: 18 and 5. The pressure range was relatively high (1090–1870 kPa) and the carbon atom concentration was kept constant at around 2×10^{18} atoms/cm³. The effects of the nature of the hydrocarbon, the oxygen addition, and the temperature on the soot induction delay time and soot yield were investigated. A second growth stage of the soot volume fraction was observed. The influence of several parameters on the existence and/or on the amplitude of this second growth seems to indicate the chemical nature of this phenomenon. Results for the soot tendency show that the soot induction delay time and soot yield depend strongly on the structure of the hydrocarbon and on the concentration of oxygen. Their study of the diesel surrogate shows that the soot inception process does not depend on synergistic effects between hydrocarbons but seems to be initiated by the constituent of the surrogate that produces soot fastest, while other constituents were consumed later during the soot growth.

Agafonov G.L. et. al. (2007) proposed a new detailed kinetic model of soot formation in shock tube pyrolysis and oxidation of aliphatic and aromatic hydrocarbons. The model is based on the comprehensive kinetic model of polyaromatic hydrocarbons (PAH) formation and growth. The gas-phase kinetic scheme was validated against the experimentally measured concentration profiles of the main gas-phase species formed

during toluene pyrolysis and H and OH radicals during benzene and phenol pyrolysis and toluene oxidation behind reflected shock waves. The model describes the main characteristics of soot formation in pyrolysis and oxidation of toluene and n-heptane oxidation under conditions typical of shock tube experiments. Both hydrocarbons have the same number of carbon atoms but different structures, which causes different behavior of the systems. The discrete Galerkin technique was applied for direct counting of the mean number of active sites formed on the surface of soot precursors and soot particles in reactions of activation, deactivation, and surface growth.

Hong et. al. (2009) investigated the influence of oxygenates on diesel soot emissions. soot formation in fuel-rich n-heptane/oxygen mixtures with added dimethyl ether, acetone, butanal, or 3-pentanone was investigated behind reflected shock waves at pressures from 20 to 30 atm and temperatures from 1600 to 1900 K. Soot formation histories were observed by simultaneously measuring the soot-induced laser light extinction at 633 nm and the light emission by soot particles at 670 nm. Uniform reflected shock conditions over the long test times needed to form soot were achieved by using a new driver insert method to modify shock tube performance. In measurements made under these uniform conditions, the soot formation window near 1700 K was found to be narrower than previously measured. A significant reduction in the overall soot yield was found with the addition of small quantities of oxygenates as well. On a per oxygen-mass basis, butanal was found to be the most effective additive in reducing soot among the oxygenates studied. It was also found that normal alkyl-group chain length in oxygenates has little impact on soot reduction.

De Iuliis et. al. (2008) focused on the development and application of the laser extinction/scattering technique in shock tube experiments. Emphasis is given to the

scattering optical arrangement for the determination of soot size growth. Results concerning the induction delay time, the soot yield and the particle diameter growth are presented for the pyrolysis of ethylene and toluene at pressure about 500 kPa and for a wide range of temperature.

Zhu et. al. (2007) investigated Catalytic oxidation of diesel soot particulate on $Ce_xZr_{1-x}O_2$ catalysts. Results indicated that Ce/Zr ratios had a significant influence on the catalytic activities. Compared with the ignition temperature (T_i) of uncatalyzed soot combustion, T_i of $Ce_{0.5}Zr_{0.5}O_2$ with the best catalytic behavior decreased by 80 °C. The reactant gas compositions (O_2 , H_2O and NO) affected the catalytic activities too. O_2 -TPD, TG-DTA and XPS characterization results showed that $Ce_xZr_{1-x}O_2$ released lattice oxygen continuously to promote the soot combustion even no gas oxygen occurred in the reaction atmosphere. The mechanisms of spill-over and reduction/oxidation functioned synergistically for soot catalytic combustion.

Hinot et. al. (2007) , performed experiments with two model soot aerosols brought into different forms of contact with Pt aerosol particles, to investigate the effectiveness of this contact in lowering the catalytic soot oxidation temperature. The contact was either generated between individual particles in the aerosol state (Pt-doped soot to simulate a fuel borne catalyst), or by sequential or simultaneous deposition of separately generated soot and Pt aerosols onto a sintered metal filter. (Formation of a soot cake on previously deposited Pt aerosol would simulate a catalyst coated diesel particle filter.) The catalytic activity was determined in all cases from temperature ramped oxidation in air of the filtered particles, and defined as the 50% conversion temperature.

It was found that Pt-doped soot and simultaneously filtered aerosols were both equally effective in reducing the oxidation temperature by up to 140–250 °C for the spark discharge soot (with 3–47 wt% Pt concentration in the soot cake), and by up to 140 °C for the pyrolysis soot (3 wt% Pt).

Conversely, the deposition of a thin soot layer of 5–10 mm thickness onto Pt, or vice versa, produced only a slight temperature reduction on the order of about 13–42 °C. These results suggest that the distance between soot and Pt particles plays a key role in promoting an effective oxidation on the filter, which is consistent with the role of Pt particles as local generators of activated oxygen.

Alexiou and Williams (1995) studied the formation of soot during the pyrolysis of argon-diluted mixtures of toluene and n-heptane and of toluene and iso-octane in a reflected-shock tube. Soot induction times and rates of formation measured at 632.8 nm by laser beam attenuation showed an Arrhenius dependence on reflected-shock temperature. The maximum in bell-shaped distribution of soot yield and concentration as a function of temperature decreased with increasing amount of n-heptane or iso-octane substituted for toluene. A kinetic model was used to explain the experimental trends and gave reasonable prediction of the experimental observations. The reduction in soot yield and concentration was attributed to the faster decomposition of the alkanes as well as to their decomposition products, which diverted the soot formation process from the more effective path of toluene pyrolysis to a slower route.

This work presents an experimental technique for the determination of the soot formation in different fuel combinations that accomplish the main target for the reduction of soot formation by using oxygenated additives. It contributes by adding a simple yet compact test rig to accomplish this task. This will give a realistic way of how researchers can accomplish soot reduction for different fuels and oxygenated additives.

CHAPTER THREE: THEORITICAL BAKGROUND

3.1 Background :

The solid and liquid particles in combustion product could be consider as soot. Soot is produced naturally by any combustion process. Soot has many bad effects in life and environment.

Soot contains up to 40 different cancer-causing chemicals and can also cause respiratory and heart diseases. It is estimated to cause two million deaths in the developing world each year – mainly among children – when emitted from wood-burning stoves in poorly ventilated houses. In Britain, research has shown that people are twice as likely to die from respiratory disease when heavily exposed to soot emitted from vehicle exhausts.

Black carbon, the component of soot that gives it its color, is thought to be the second largest cause of global warming after carbon dioxide. Formed through incomplete combustion of fossil fuels, wood and vegetation, it delivers a double whammy. While in the air, it is spread around the globe by the wind, and helps to heat the atmosphere by absorbing and releasing solar radiation. When soot falls out soot darkens snow and ice, at the poles or high in mountains, reducing its ability to reflect sunlight. As a result it melts more quickly, and exposes more dark land or water which absorbs even more energy, and so increases warming.

3.2 Soot visual detection:

Soot is solid substance consisting of roughly eight parts carbon and one part hydrogen (Tree 2007). Soot is produced from many sources such as burning coal, diesel, wood etc.

As shown in Fig 3.1 and Fig 3.2, in order to measure soot formation, a customized filter has been prepared which is able to absorb the soot produced by the combustion.



Figure 3.1 Inner grade of the filter used



Figure 3.2 Customized filter

3.3 Temperature measuring principle:

Temperature has the greatest effect of any parameter on the soot formation due to increase all of the reaction rates involved in soot formation and oxidation. Soot inception begins at around a temperature 200°C , while of burnout ceases below 300°C . As temperature is increased the rate of oxidation increases more rapidly than the rate of formation. In the experimental work temperature measurement was carried out using k-type thermocouple as shown in Fig 3.3. It is located within drive section, and hence the temperature will measure the ignition temperature.



Figure 3.3 Thermocouple in drive section

3.4 Pressure measuring principle

The pressure and temperature are related by the ideal gas law, and hence when temperature increase the pressure will rise. Further, changing the pressure experienced by a flame often results in changes in the temperature, flow velocity, flame structure, and thermal diffusivity. Thus the effects of pressure on soot can be difficult to isolate. In this experimental work pressure will be measured by using dynamic pressure sensor as shown in Fig 3.4, which is in the drive section. This technique will measure the ignition pressure in the drive section.



Figure 3.4 pressure sensor

3.5 Fuel preparation:

The fuel sample were prepared in the lab(Tamer 2010). For illustration purpose summery of the fuel procedure will be given below :

Biofuel preparation:

A clean and safe area away from flammable substances must be available before starting the preparation 20-22% amount of methanol is needed for every amount of oil. 0.55% of NaOH is needed also for every amount of oil. For example: for 10 liters of oil it is required to have 2 liters of methanol and 55g of NaOH. Oil is heated up to 130 °C. At the same time a mixture of methanol and NaOH is prepared which is called Methodixe. This substance is then mixed with heated oil for 24 hours. The

resultant mixture will contain glycerine at the bottom and biofuel at the top of the mixing area. Removing glycerine from the bottom and by this will produce biofuel. But this biofuel still contains methanol and glycerine. It can be removed by adding distilled water that acts as a magnet to these substances because methanol is similar to water more than oil. This water will flow upward where it can be removed easily and the biofuel is dried by air for more purification.

Emulsified fuel preparation:

The water addition ranges between 0-20% .The mixing obtained by an homogenizer device. Water particles become micro-explode due to the discrepancy of the boiling point between the diesel and the water (boiling point of water 100⁰C, boiling point of the diesel 185⁰C) (Appl 2010) so that the emulsion fuel drops divided into finer particles and this leads to an increase the volatility of the fuel and hence the combustion efficiency.

In the next chapter, appropriate combination of measuring equipment to verify theory discussed . Building of the testing facility as well as its performance and reliability will be performed.

CHAPTER FOUR: TESTING FACILITY AND MEASUREMENTS

In any experimental work, the development of a testing setup that is able to deliver reliable results is the aid of any research. This work was developed step by step to generate acceptable setup which will deliver satisfactory results.

4.1 Selection of shock tube material:

As a first step, some of the calculations have been done in order to determine the type of material to be used. This is based on standard design and combustion theory, which is used to determine the mass of fuel and oxygen required .

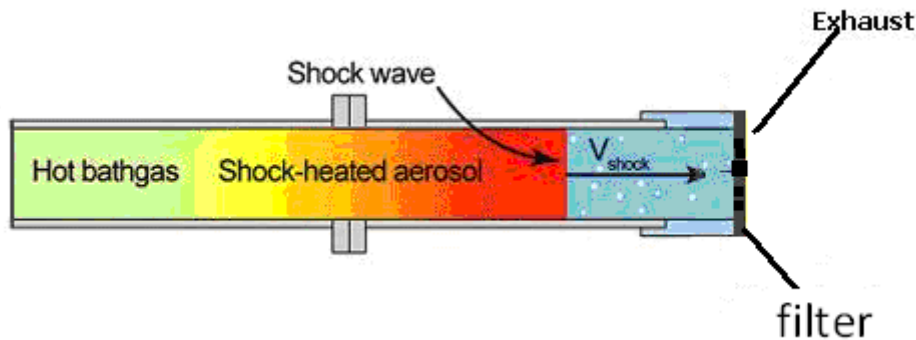


Figure 4.1: shock tube sketch

The thickness and type of material for the shock tube has been selected using ASME B 16.5a 1998 standard as per the following equations:

$$t = (P \cdot R_o) / (SE + 0.4P)$$

(4.1)

$$t = (500 \cdot 1.5) / (1266.18 \cdot 1 + 0.4 \cdot 500) = 0.51" = 12.95\text{mm}$$

For a spherical head

$$t = (P * Do) / (2SE + 1.8P)$$

(4.2)

It may be written as:

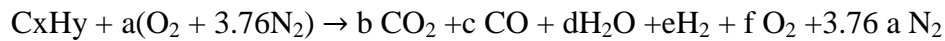
$$t = \frac{500 * 3}{2 * 1266.18 * 1 + 1.8 * 500} = 0.44$$

$$= 11.18\text{mm}$$

Where (t) is the thickness of the shock tube, (P) is the pressure (500 bar), (Do) is the outer diameter (3"), (S) is material allowed strength, (E) is joint efficiency, as per standards.

The amount of diesel used in the shock tube depends on size of shock tube, which is 1600mm long with Inner diameter=38mm.

The combustion of an arbitrary hydrocarbon with our simplified air can be represented by



...(4.3)

The lap conditions are T=25 °C, Pressure=0.92 bar.

$$\Rightarrow \text{calculate air fuel ratio} = \frac{A}{F}$$

Where $a = x + y / 4 \dots \dots \dots \phi = 1$

in table (B.2) from An introduction to combustion book $x=10.8$, $y=18.7$

$$a = x + \frac{y}{4} = 15.475$$

Volume of tube

$$v = \frac{\pi}{4} * D^2 * L$$

$$v = \frac{\pi}{4} * (0.038)^2 * (1.600) = 1.8e^{-3}m^3$$

$$\rho = 1.2 \text{ kg/m}^3$$

$$\text{Mass of air} = 1.8e^{-3} * 1.25 = 2.2e^{-3}$$

$$\frac{A}{F} = C * \text{Molecular weight of air} / \text{Molecular weight of fuel}$$

$$\frac{A}{F} = \text{mass} * \rho / \text{mass of fuel}$$

$$14.33 = 2.2e^{-3} / \text{mass of fuel}$$

Where $C = 4.76 * a$

Mass of fuel = 0.15 gram

In order to calculate oxygen mass, the following procedure is followed:

$m_{O_2 \text{ total}} = m_{O_2 \text{ original}} + m_{O_2 \text{ supply}}$ at certain pressure

$$\frac{O_2}{F} = C * \text{Molecular weight of oxygen} / \text{Molecular weight of fuel}$$

$$\frac{O_2}{F} = 1 * a * \frac{MW_{O_2}}{MW_{fuel}}$$

$$\frac{O_2}{F} = 15.075 * \frac{28.85}{148.6} = 2.93$$

Mass of oxygen = $2.93 * 0.15 = 0.44$ gram at constant pressure = 1.5 bar.

Then the selected type of material in this experimental work will be "Seamless pipe

Schedule 80) based on tables in the ASME standard mentioned above. This is

considered the best type and tolerant to possible high pressure and temperature.

4.2 Shock tube:

A shock tube is a device used primarily to study gas phase combustion reactions. A simple shock tube is a tube, rectangular or circular in cross-section, usually constructed of metal, in which a gas at low pressure and a gas at high pressure are separated using some form of diaphragm. This diaphragm suddenly bursts open under predetermined conditions to produce a wave propagating through the low pressure section. The shock that eventually forms increases the temperature and pressure of the test gas and induces a flow in the direction of the shock wave. Observations can be made in the flow behind the incident front or take advantage of the longer testing times and vastly enhanced pressures and temperatures behind the reflected wave.

As shown in Fig 4.2, the shock tube consist of two main parts :

The first one is the drive section with length of 1600 mm and inner diameter of 38 mm and contain 4 holes. The first hole is for pressure gauge, second hole is for spark plug, third hole is for thermometer and the fourth hole is for feeding gas. As shown in Fig. 4.2.

The second part of shock tube is the driven section, 1600 mm length and 38 mm inner diameter contains only a customized filter at the end.



Figure 4.2: Shock tube sketch

In this shock tube, the drive section has closed end but the driven is open as shown in Fig 4.3. Also the drive and driven section has been linked by flange coupling as shown in Fig 4.4 and Fig 4.5.



Figure 4.3: Closed end in the drive section



Figure 4.4: Flange coupling

The flange design contains a membrane made of copper (0.05 mm thickness). This membrane is installed with a gasket as it resists high temperature almost 700 °C which is shown in fig 4.5.



Figure 4.5: Shock tube membrane

To be sure that the membrane will be cracked in the pressure range of the combustion testes, air supply tests have been made at various pressures. It was found that the diaphragm cracks at a pressure of 5 bars for 0.05mm thickness shim diaphragm, and the expected pressure of cracking the 0.1mm thickness shim diaphragm was 10 bars. The explosion pressures range was 7-10 bars, this was related to the type of diesel and the type of diaphragm material specification.

4.3 Electric heater coil:

Having introduced the fuel and air in to the shock tube, which are at room temperature. This mixture has to be heated up to vaporize the diesel fuel and hence ignite the mixture. Three electric heaters were rolled along the tube, where each requires a power of 3 kW. It have been installed in spiral pattern long the tube.



Figure 4.6: Electric heater coil installation around shock tube

After installing the electric heater coil around the tube and connecting it to electricity, heat transmitted through the tube material into the diesel in the drive section. This caused the diesel to ignite and the process of shock wave started. The temperature of the ignition as per the temperature digital thermometer was approximately 300 °C.



Figure 4.7: Heating shock tube

Finally to finish preparing the test rig. Gas connections were prepared, as it must be a wiring far from the heat and we can control the amount of gas through the control valve.

Oxygen was provided to the experiment in order to help in ignition phase.

4.4 Measuring devices and measurements:

K-type thermometer is used to measure the process temperature inside the tube where it has the following features:

- i. Can match any standard type K sensor.
- ii. Fitted with standard K probe socket.
- iii. LCD display provides low power consumption.
- iv. LSI-circuit use provides high reliability and durability.
- v. High accuracy and wide measurement range.
- vi. Compact, lightweight, and excellent operation.
- vii. Circuit used high quality multi turns VR for keeping high accuracy and reliability.



Figure 4.8: Digital thermometer

After preparing the temperature measurement, pressure sensor is used to measure the pressure of explosion in the drive section. The range of this pressure sensor varies between 0 to 25 bar with maximum working temperature 100 °C.

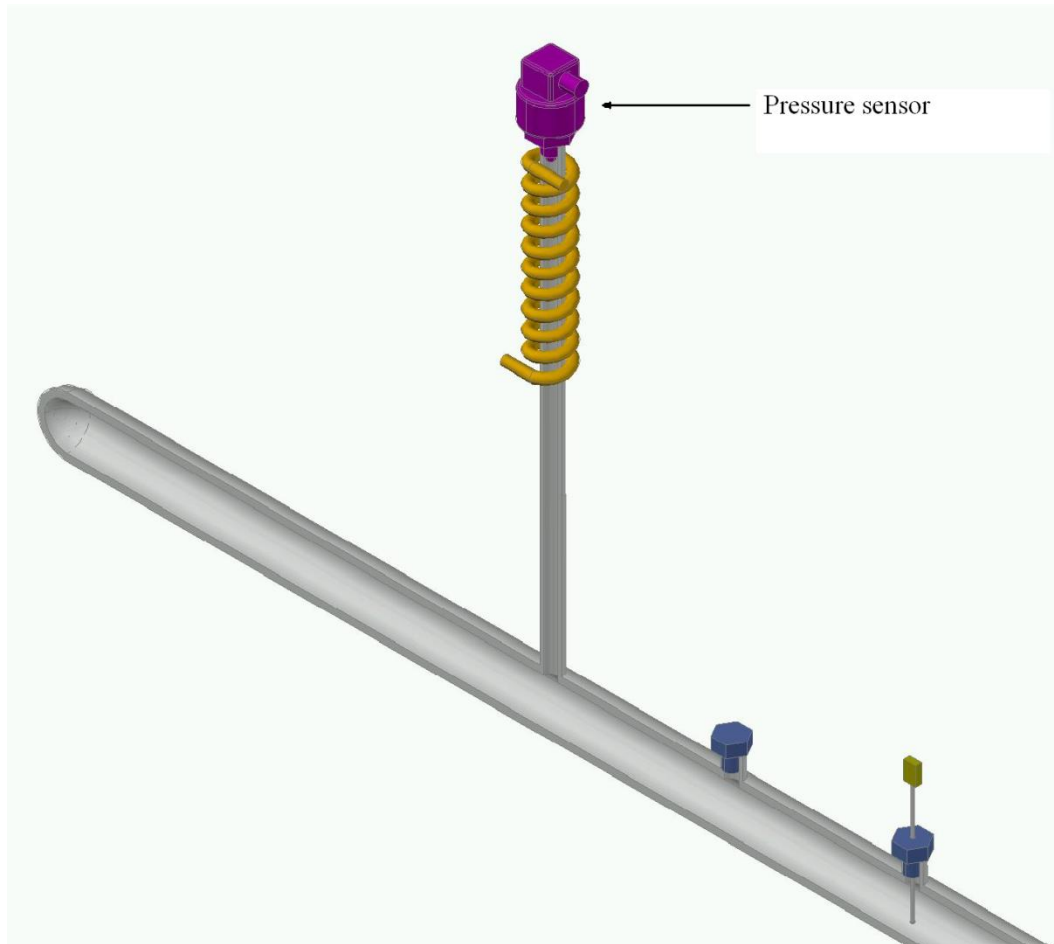


Figure 4.9: Pressure sensor setup

Signals received from the pressure sensor are transmitted to the computer through data acquisition card with a compatible program.

The features of pressure sensor used are:

- i. Corrosion resistant stainless steel design
- ii. Medium wetted parts of stainless steel
- iii. No internal sealing elements
- iv. Pressure connection G1/4 B
- v. High peak pressure resistance
- vi. High alternating load resistance
- vii. High long-term stability
- viii. For dynamic and static measurements



Figure 4.10: Pressure sensor

CHAPTER FIVE: EXPERIMENTAL PROCEDURE

After completing all necessary connections and verification. The combustible mixture is prepared in the appropriate A/F ratio and then it is introduced into the drive section, then mixture heated up to a point of converting liquid phase to gases phase. The change from the liquid phase to gas phase will cause self-ignition and explosion with the assistance of oxygen which produces the exhaust. Tests were conducted for three types of mixtures: diesel, biofuel and emulsified fuel all mixed with the additives ethanol, methanol, and acetone. The first mixture is diesel with the additives. In this step the soot formation in the diesel has been studied together with the effect of additives.

Table 5.1: Samples matrix

	Diesel	Biofuel	Emulsified fuel
No additive	Sample 1	Sample 5	Sample 9
Methanol	Sample 2	Sample 6	Sample 10
Ethanol	Sample 3	Sample 7	Sample 11
Acetone	Sample 4	Sample 8	Sample 12

Table 5.1 show the steps of fuel testing before and after additives, there are two kind of testing:

The first test of each set in table (5.1) was carried out without additives, and the soot formation was measured for each pure fuel. The second test was carried out using each fuel with additives, finally the effects of each additives on soot formation reduction were compared together.

The soot was measured by using a customized filter to give soot accumulation where the effect of additives in soot formation is measured. The filter is placed in the driven section where a visual check will give an indication of soot formation. For example, if the soot on the filter is dark then it gives the indication of large accumulation of soot. In the same manner if it is light, this gives an indication that soot is little.



Figure 5.1: Filter placement at the tip of driven section

This test rig has been assembled in order to perform the specific task for soot detection through visual measurement. Each additive caused a different amount of soot; this will be shown in the result chapter. It is to be noted that the amount of the three additives to each fuel was fixed at 20%.

CHAPTER SIX: EXPERIEMNTAL RESULTS

The following results are grouped into four main categories, based on the quantity of soot formed on the filter.

As shown in Fig 6.1 and as expected soot formation was maximum where pure diesel was burn, followed by emulsified fuel and biofuel respectively. This is because diesel fuel is made up of a blend of heavy hydrocarbons that contains large number of carbon atom (Tree,2007).

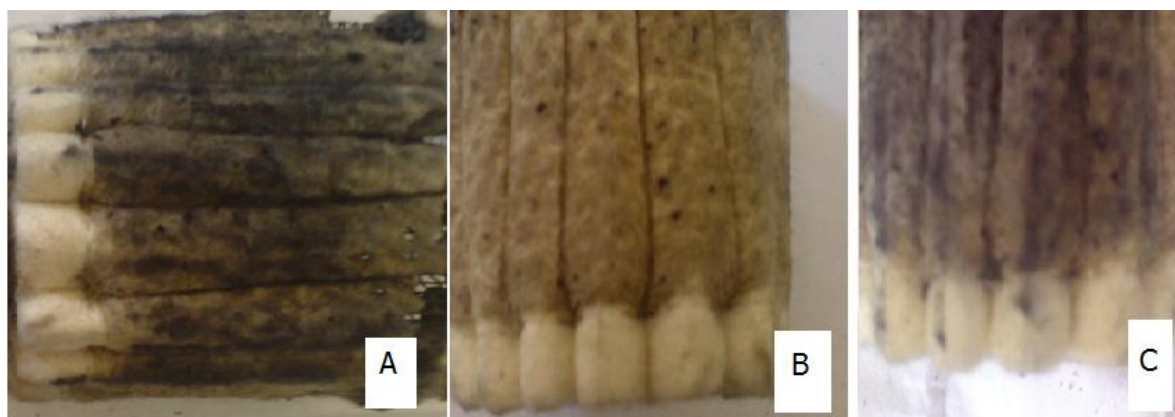


Figure 6.1: Sample 1 (A: Diesel) vs. sample 5 (B: Biofuel) .sample 9 (C: Emulsified fuel)

The second category is the mixture of fuels with methanol which showed the least soot formation based on visual identification. It is clear that fuel composition influences the amount of soot produced in combustion process. Since methanol contains low carbon structure, also it contains oxygen that enhances the burning and hence the reduction of soot production.

Fig 6-2 shows the filter after biofuel and methanol mixture was burned, as indicated by the colour of the filter, the soot formation is minimum.



Figure 6.2: sample 6 (biofuel with methanol)

Fig 6.3, in the case of burning of fuels with methanol additive. As expected soot formation was maximum when pure diesel and methanol were burn, followed by emulsified fuel and biofuel respectively. This is because diesel fuel is made up of a blend of heavy hydrocarbons that contains large number of carbon atom .

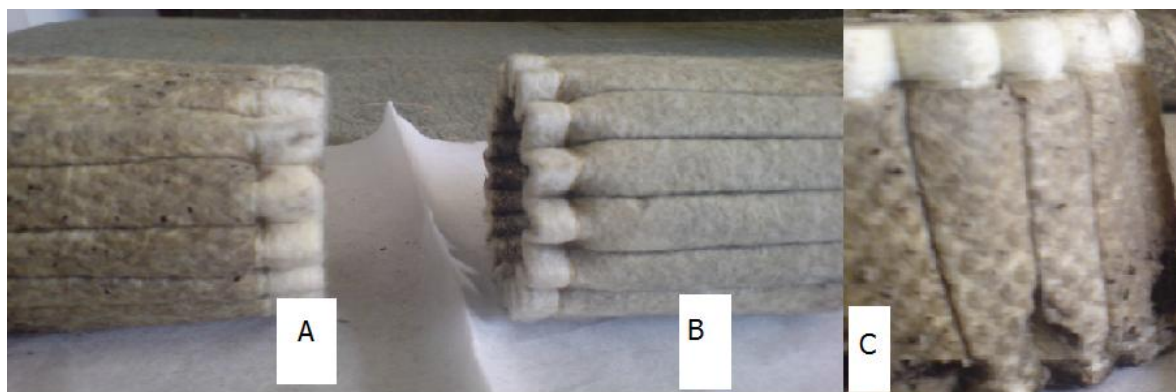


Figure 6.3: Sample 2 (A: Diesel) vs. sample 6 (B: Biofuel). sample 10 (C: Emulsified)

The next category is the mixture of fuels with ethanol. It can be seen that the degree of soot formation higher that formed when methanol added. As shown in Fig 6.4 and

as expected soot formation was maximum when pure diesel was burned, followed by emulsified fuel and biofuel respectively.

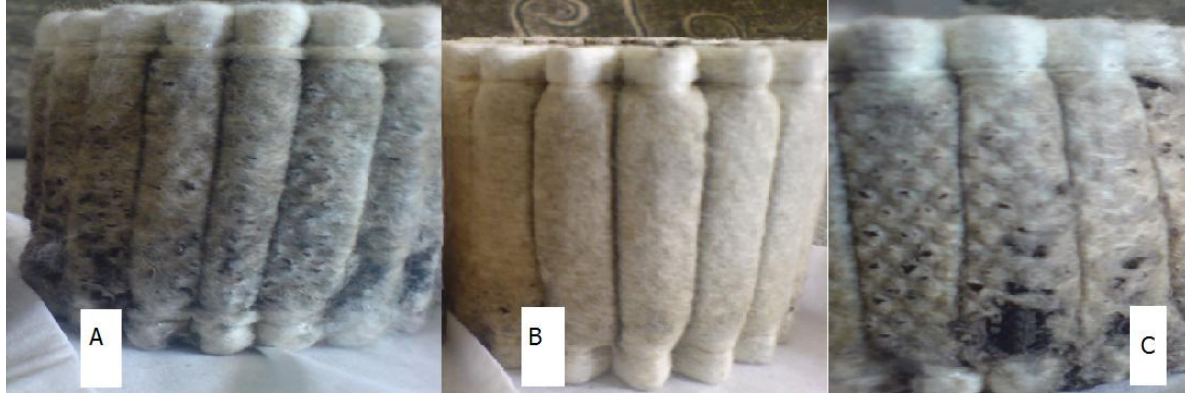


Figure 6.4: Sample 3 (A: Diesel)vs. sample 7 (B: Biofuel). sample 11(C: Emulsified)

As shown in Fig 6.5 and Fig 6.6 ,the last category of this study was mixture of fuels and acetone. As indicated the soot formation was mixture when acetone was added. Similarly soot formation was maximum when diesel with acetone was burned followed by mixture of emulsified with acetone and minimum formation when biofuel and acetone was burned.

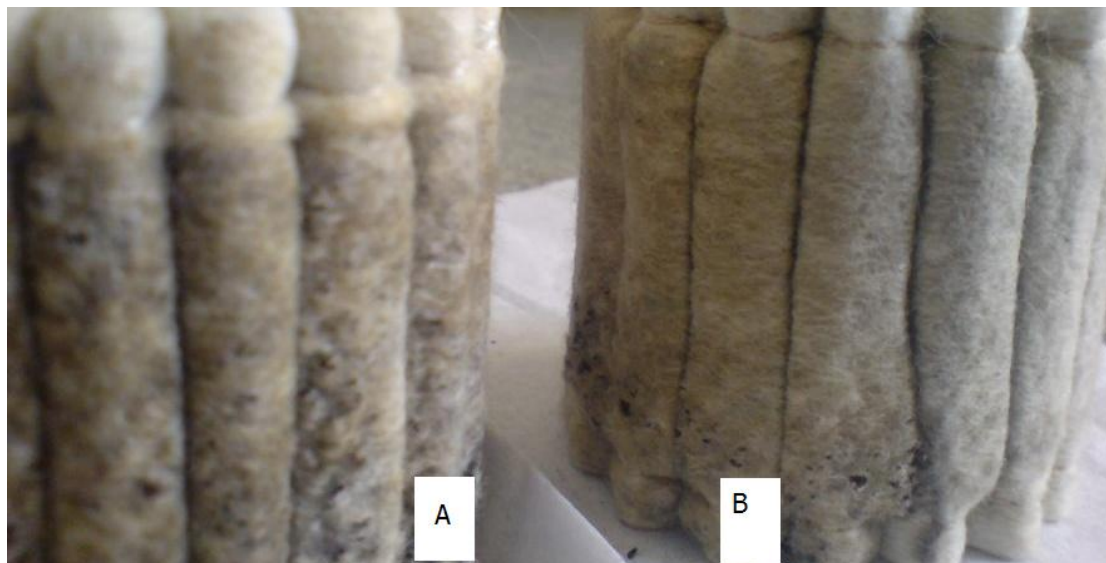


Figure 6.5: Sample 12 (A: Emulsified fuel) vs. sample 8 (B: Biofuel)

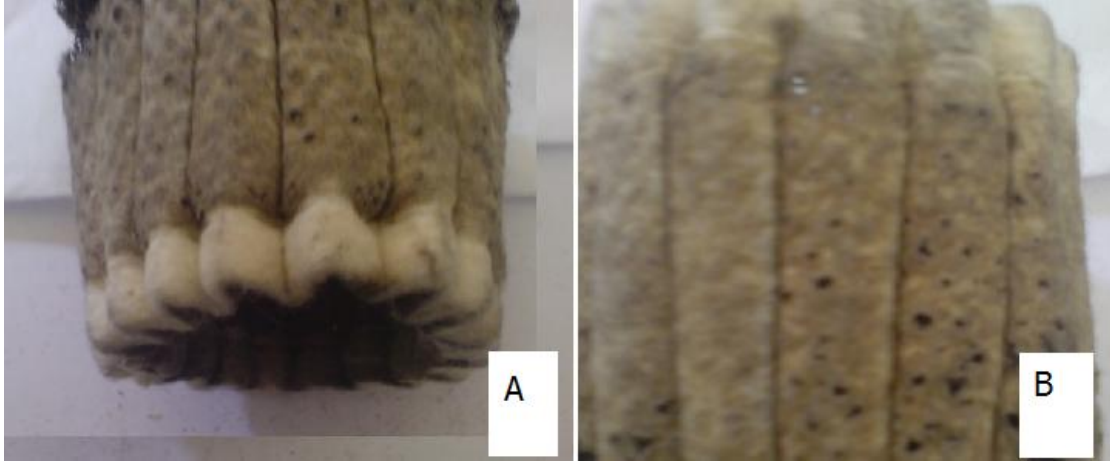


Figure 6.6: Sample 8 (A: Biofuel) vs. sample 4 (B: Diesel)



Figure 6.7: Sample 12: emulsified fuel mixed with acetone



Figure 6.8: Sample 4: Diesel with acetone mixture

The soot formation and the effect of the additives on each type of fuel on its formation is shown in Fig 6.9 and table 6.1. As shown in Fig 6.9 all samples are listed along the horizontal axis and the black vertical column represent the degree of soot formation in table 6.1.

Table 6.1: Soot comparison matrix based on colour detection

	Diesel	Bio fuel	Emulsified fuel
No additive	Sample 1	Sample 5	Sample 9
Methanol	Sample 2	Sample 6	Sample 10
Ethanol	Sample 3	Sample 7	Sample 11
Acetone	Sample 4	Sample 8	Sample 12

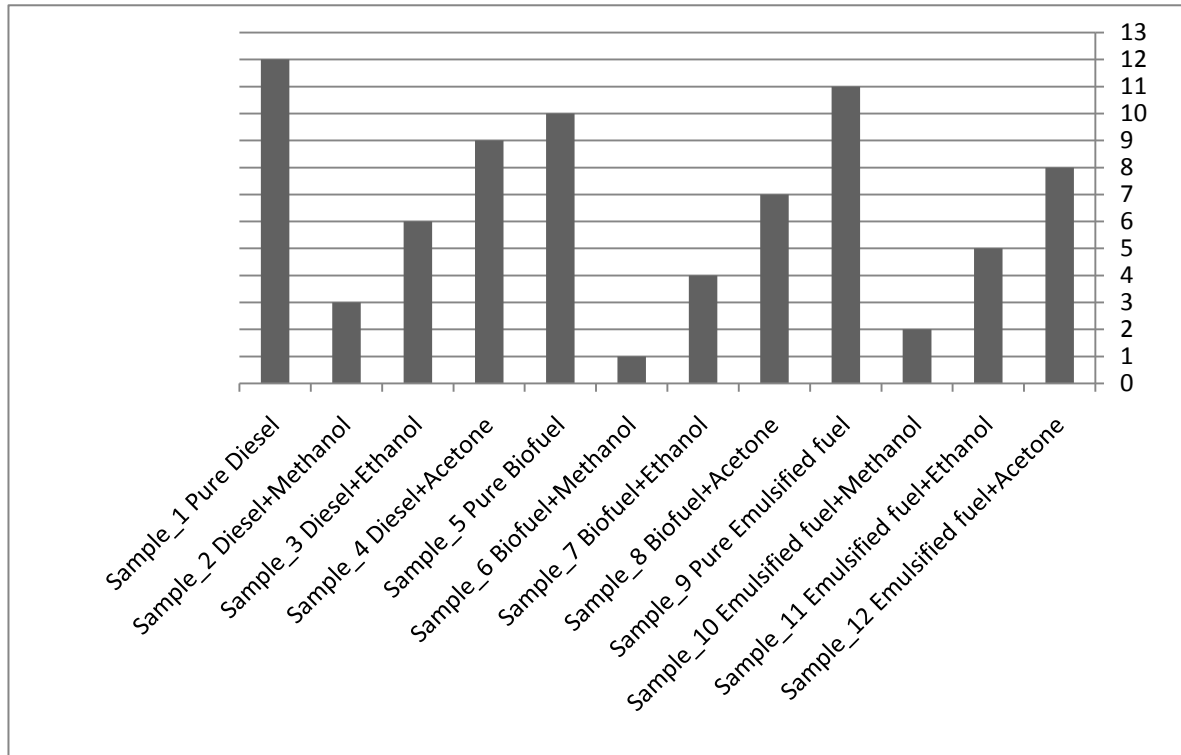


Figure 6.9: Comparison between all samples based on (1-12) scale

CHAPTER SEVEN: CONCLUSION AND FINAL REMARKS

This work was carried to find effect of oxygenated additives on the formation of soot emitted during the combustion of diesel, biofuel and emulsified fuel. From this work it may be concluded that :-

1. Soot formation is maximum when pure diesel is burned and minimum when biofuel is burned.
2. Methanol has the maximum effect on soot reduction when added to all three types of fuel. With minimum reduction of soot when added to biofuel.
3. Acetone has minimum effect on soot reduction when added to all fuel. With minimum effect when added to diesel fuel.

REFERENCES

- Alexiou, A. and Williams, A. (1995), “Soot formation in shock-tube pyrolysis of toluene *n*-heptane and toluene *iso*-octane mixtures”, **Fuel**, 74(2), 153-158.
- De Iuliis, S., Chaumeix, N., Idir, M. and Paillard, E. (2008), “Scattering / extinction measurements of soot formation in a shock tube”, **Experimental Thermal and Fluid Science**, 32, 1354–1362.
- G.L., Agafonov, G. L., Naydenova, I., Vlasov, P., A.Warnatz, J., (2007), “Detailed kinetic modeling of soot formation in shock tube pyrolysis and oxidation of toluene and *n*-heptane”, **Proceedings of the Combustion Institute**, 31, 575–583.
- Hong, Z., Davidson, D.F., Vasu, S.S. and Hanson, R.K. (2009), “The effect of oxygenates on soot formation in rich heptane mixtures: A shock tube study”, **Fuel**, 88, 1901–1906.
- Hinot, K., Burtscher, H., Weber, A.P. and Kasper, G., (2007), “The effect of the contact between platinum and soot particles on the catalytic oxidation of soot deposits on a diesel particle filter”. **Applied Catalysis B: Environmental**, 71, 271–278.
- Mathieu, O., Djebaili-Chaumeix, N., Paillard, C. and Douce, F., (2009), “Experimental study of soot formation from a diesel fuel surrogate in a shock tube”, **Combustion and Flame**, 156, 1576–1586.
- Tamer Ewimer”. **Optimization study for performance of compression ignition engines powered by emulsified fuels**,(2010), thesis of master degree.
- Turns, S., “**An introduction to combustion: concepts and applications**”, (2000), 2nd edition, McGraw – Hill higher education.
- Zhua, L., Yu, J. and Wang, X., (2007), “Oxidation treatment of diesel soot particulate on $Ce_xZr_{1-x}O_2$ ”, **Journal of Hazardous Materials**, 140, 205–210.

APPENDICES

APPENDIX (A): Rating for group 2.2 material

ASME B16.5a-1998

PIPE FLANGES AND FLANGED FITTINGS

TABLE RATINGS FOR GROUP 2.2 MATERIALS

Nominal Designation	Forgings	Castings	Plates
16Cr-12Ni-2Mo	A 182 Gr. F316 (1) A 182 Gr. F316H	A 351 Gr. CF3M (2) A 351 Gr. CF8M (1)	A 240 Gr. 316 (1) A 240 Gr. 316H
18Cr-13Ni-3Mo			A 240 Gr. 317 (1)
19Cr-10Ni-3Mo		A 351 Gr. CG8M (3)	

NOTES:

- (1) At temperatures over 1000°F, use only when the carbon content is 0.04% or higher.
(2) Not to be used over 850°F.
(3) Not to be used over 1000°F.

WORKING PRESSURES BY CLASSES, psig

Class Temp., °F	150	300	400	600	900	1500	2500
-20 to 100	275	720	960	1440	2160	3600	6000
200	235	620	825	1240	1860	3095	5160
300	215	560	745	1120	1680	2795	4660
400	195	515	685	1025	1540	2570	4280
500	170	480	635	955	1435	2390	3980
600	140	450	600	900	1355	2255	3760
650	125	445	590	890	1330	2220	3700
700	110	430	580	870	1305	2170	3620
750	95	425	570	855	1280	2135	3560
800	80	420	565	845	1265	2110	3520
850	65	420	555	835	1255	2090	3480
900	50	415	555	830	1245	2075	3460
950	35	385	515	775	1160	1930	3220
1000	20	350	465	700	1050	1750	2915
1050	...	345	460	685	1030	1720	2865
1100	...	305	405	610	915	1525	2545
1150	...	235	315	475	710	1185	1970
1200	...	185	245	370	555	925	1545
1250	...	145	195	295	440	735	1230
1300	...	115	155	235	350	585	970
1350	...	95	130	190	290	480	800
1400	...	75	100	150	225	380	630
1450	...	60	80	115	175	290	485
1500	...	40	55	85	125	205	345

APPENDIX (B): List of material specification

ASME B16.5a-1998

PIPE FLANGES AND FLANGED FITTINGS

(a) TABLE LIST OF MATERIAL SPECIFICATIONS

Material Group	Nominal Designation	Pressure-Temperature Rating Table	Applicable ASTM Specifications ¹		
			Forgings	Castings	Plates
1.1	C-Si C-Mn-Si C-Mn-Si-V	2-1.1	A 105 A 350 Gr. LF2 A 350 Gr. LF6 Cl. 1	A 216 Gr. WCB	A 515 Gr. 70 A 516 Gr. 70 A 537 Cl. 1
1.2	C-Mn-Si C-Mn-Si-V 2½Ni 3½Ni	2-1.2	 A 350 Gr. LF6 Cl. 2 A 350 Gr. LF3	A 216 Gr. WCC A 352 Gr. LCC A 352 Gr. LC2 A 352 Gr. LC3	 A 203 Gr. B A 203 Gr. E
1.3	C-Si C-Mn-Si 2½Ni 3½Ni	2-1.3		A 352 Gr. LCB	A 515 Gr. 65 A 516 Gr. 65 A 203 Gr. A A 203 Gr. D
1.4	C-Si C-Mn-Si	2-1.4	A 350 Gr. LF1 Cl. 1		A 515 Gr. 60 A 516 Gr. 60
1.5	C-½Mo	2-1.5	A 182 Gr. F1	A 217 Gr. WC1 A 352 Gr. LC1	A 204 Gr. A A 204 Gr. B
1.7	C-½Mo ½Cr-½Mo Ni-½Cr-½Mo ¾Ni-¾Cr-1Mo	2-1.7	A 182 Gr. F2	 A 217 Gr. WC4 A 217 Gr. WC5	A 204 Gr. C
1.9	1Cr-½Mo 1¼Cr-½Mo 1¼Cr-½Mo-Si	2-1.9	A 182 Gr. F12 Cl. 2 A 182 Gr. F11 Cl. 2	A 217 Gr. WC6	A 387 Gr. 11 Cl. 2
1.10	2¼Cr-1Mo	2-1.10	A 182 Gr. F22 Cl. 3	A 217 Gr. WC9	A 387 Gr. 22 Cl. 2
1.13	5Cr-½Mo	2-1.13	A 182 Gr. F5 A 182 Gr. F5a	A 217 Gr. C5	
1.14	9Cr-1Mo	2-1.14	A 182 Gr. F9	A 217 Gr. C12	
1.15	9Cr-1Mo-V	2-1.15	A 182 Gr. F91	A 217 Gr. C12A	A 387 Gr. 91 Cl. 2
2.1	18Cr-8Ni	2-2.1	A 182 Gr. F304 A 182 Gr. F304H	A 351 Gr. CF3 A 351 Gr. CF8	A 240 Gr. 304 A 240 Gr. 304H
2.2	16Cr-12Ni-2Mo 18Cr-13Ni-3Mo 19Cr-10Ni-3Mo	2-2.2	A 182 Gr. F316 A 182 Gr. F316H	A 351 Gr. CF3M A 351 Gr. CF8M A 351 Gr. CG8M	A 240 Gr. 316 A 240 Gr. 316H A 240 Gr. 317
2.3	18Cr-8Ni 16Cr-12Ni-2Mo	2-2.3	A 192 Gr. F304L A 182 Gr. F316L		A 240 Gr. 304L A 240 Gr. 316L
2.4	18Cr-10Ni-Ti	2-2.4	A 182 Gr. F321 A 182 Gr. F321H		A 240 Gr. 321 A 240 Gr. 321H

APPENDIX (C): List of bolting specification

PIPE FLANGES AND FLANGED FITTINGS

ASME B16.5-1996

TABLE LIST OF BOLTING SPECIFICATIONS
Applicable ASTM Specifications¹⁵

Bolting Materials [Note (1)]											
High Strength [Note (2)]			Intermediate Strength [Note (3)]			Low Strength [Note (4)]			Nickel and Special Alloy [Note (5)]		
Spec. No.	Grade	Notes	Spec. No.	Grade	Notes	Spec. No.	Grade	Notes	Spec. No.	Grade	Notes
A 193	B7	...	A 193	B5	...	A 193	B8 Cl.1	(5)	B 164	...	(7)(8)(9)
A 193	B16	...	A 193	B6	...	A 193	B8C Cl.1	(6)	B 166	...	(7)(8)(9)
A 320	L7	(10)	A 193	B8X	...	A 193	B8M Cl.1	(6)	B 335	N10865	(7)
A 320	L7A	(10)	A 193	B7M	...	A 193	B8T Cl.1	(6)	B 408	...	(7)(8)(9)
A 320	L7B	(10)	A 193	B8 Cl.2	(11)	A 193	B8A	(6)	B 473	...	(7)
A 320	L7C	(10)	A 193	B8C Cl.2	(11)	A 193	B8CA	(6)	B 574	N10276	(7)
A 320	L43	(10)	A 193	B8M Cl.2	(11)	A 193	B8MA	(6)			
			A 193	B8T Cl.2	(11)	A 193	B8TA	(6)			
A 354	BC	...	A 320	B8 Cl.2	(11)	A 307	B	(12)			
A 354	BD	...	A 320	B8C Cl.2	(11)						
			A 320	B8F Cl.2	(11)	A 320	B8 Cl.1	(6)			
A 540	B21	...	A 320	B8M Cl.2	(11)	A 320	B8C Cl.1	(6)			
A 540	B22	...	A 320	B8T Cl.2	(11)	A 320	B8M Cl.1	(6)			
A 540	B23	...	A 449	...	(13)	A 320	B8T Cl.1	(6)			
A 540	B24	...									
			A 453	651	(14)						
			A 453	660	(14)						

GENERAL NOTE: Bolting material shall not be used beyond temperature limits specified in the governing code.

NOTES:

- (1) Repair welding of bolting material is prohibited.
- (2) These bolting materials may be used with all listed materials and gaskets.
- (3) These bolting materials may be used with all listed materials and gaskets, provided it has been verified that a sealed joint can be maintained under rated working pressure and temperature.
- (4) These bolting materials may be used with all listed materials but are limited to Classes 150 and 300 joints. See para. 5.4.1 for required gasket practices.
- (5) These materials may be used as bolting with comparable nickel and special alloy parts.
- (6) This austenitic stainless material has been carbide solution treated but not strain hardened. Use A 194 nuts of corresponding material.
- (7) Nuts may be machined from the same material or may be of a compatible grade of ASTM A 194.
- (8) Maximum operating temperature is arbitrarily set at 500°F, unless material has been annealed, solution annealed, or hot finished because hard temper adversely affects design stress in the creep rupture range.
- (9) Forging quality not permitted unless the producer last heating or working these parts tests them as required for other permitted conditions in the same specification and certifies their final tensile, yield, and elongation properties to equal or exceed the requirements for one of the other permitted conditions.
- (10) This ferritic material is intended for low temperature service. Use A 194 Grade 4 or Grade 7 nuts.
- (11) This austenitic stainless material has been carbide solution treated and strain hardened. Use A 194 nuts of corresponding material.
- (12) This carbon steel fastener shall not be used above 400°F or below -20°F. See also Note (4). Bolts with drilled or undersized heads shall not be used.
- (13) Acceptable nuts for use with quenched and tempered bolts are A 194 Grades 2 and 2H. Mechanical property requirements for studs shall be the same as those for bolts.
- (14) This special alloy is intended for high temperature service with austenitic stainless steel.
- (15) ASME Boiler and Pressure Vessel Code, Section II materials, which also meet the requirements of the listed ASTM specifications, may also be used.

APPENDIX (D): Ratings for group 2.1 materials

PIPE FLANGES AND FLANGED FITTINGS

ASME B16.5a-1998

TABLE RATINGS FOR GROUP 2.1 MATERIALS

Nominal Designation	Forgings	Castings	Plates
18Cr-8Ni	A 182 Gr. F304 (1)	A 351 Gr. CF3 (2)	A 240 Gr. 304 (1)
	A 182 Gr. F304H	A 351 Gr. CF8 (1)	A 240 Gr. 304H

NOTES:

(1) At temperatures over 1000°F, use only when the carbon content is 0.04% or higher.

(2) Not to be used over 800°F.

WORKING PRESSURES BY CLASSES, psig

Class Temp., °F	150	300	400	600	900	1500	2500
-20 to 100	275	720	960	1440	2160	3600	6000
200	230	600	800	1200	1800	3000	5000
300	205	540	720	1080	1620	2700	4500
400	190	495	660	995	1490	2485	4140
500	170	465	620	930	1395	2330	3880
600	140	435	580	875	1310	2185	3640
650	125	430	575	860	1290	2150	3580
700	110	425	565	850	1275	2125	3540
750	95	415	555	830	1245	2075	3460
800	80	405	540	805	1210	2015	3360
850	65	395	530	790	1190	1980	3300
900	50	390	520	780	1165	1945	3240
950	35	380	510	765	1145	1910	3180
1000	20	320	430	640	965	1605	2675
1050	...	310	410	615	925	1545	2570
1100	...	255	345	515	770	1285	2145
1150	...	200	265	400	595	995	1655
1200	...	155	205	310	465	770	1285
1250	...	115	150	225	340	565	945
1300	...	85	115	170	255	430	715
1350	...	60	80	125	185	310	515
1400	...	50	65	90	145	240	400
1450	...	35	45	70	105	170	285
1500	...	25	35	55	80	135	230

APPENDIX (E): Curve fit coefficient for fuel specification heat

$$\bar{c}_p \text{ (kJ/kmol-K)} = 4.184(a_1 + a_2\theta + a_3\theta^2 + a_4\theta^3 + a_5\theta^{-2}),$$

$$\bar{h}^\circ \text{ (kJ/kmol)} = 4184(a_1\theta + a_2\theta^2/2 + a_3\theta^3/3 + a_4\theta^4/4 - a_5\theta^{-1} + a_6),$$

$$\text{where } \theta \equiv T \text{ (K)/1000}$$

Formula	Fuel	MW	a_1	a_2	a_3	a_4	a_5	a_6	a_8^b
CH ₄	Methane	16.043	-0.29149	26.327	-10.610	1.5656	0.16573	-18.331	4.300
C ₃ H ₈	Propane	44.096	-1.4867	74.339	-39.065	8.0543	0.01219	-27.313	8.852
C ₆ H ₁₄	Hexane	86.177	-20.777	210.48	-164.125	52.832	0.56635	-39.836	15.611
C ₈ H ₁₈	Isooctane	114.230	-0.55313	181.62	-97.787	20.402	-0.03095	-60.751	20.232
CH ₃ OH	Methanol	32.040	-2.7059	44.168	-27.501	7.2193	0.20299	-48.288	5.3375
C ₂ H ₅ OH	Ethanol	46.07	6.990	39.741	-11.926	0	0	-60.214	7.6135
C _{8.26} H _{15.5}	Gasoline	114.8	-24.078	256.63	-201.68	64.750	0.5808	-27.562	17.792
C _{7.76} H _{13.1}		106.4	-22.501	227.99	-177.26	56.048	0.4845	-17.578	15.232
C _{10.8} H _{18.7}	Diesel	148.6	-9.1063	246.97	-143.74	32.329	0.0518	-50.128	23.514

^aSOURCE: From Heywood, J. B., *Internal Combustion Engine Fundamentals*, McGraw-Hill, New York, 1988, by permission of McGraw-Hill, Inc.

^bTo obtain 0 K reference state for enthalpy, add a_8 to a_6 .

APPENDIX (F): Selection the material of high maximum allowable

stress

SECTION I; SECTION III, CLASS 2 AND 3;* SECTION VIII, DIVISION 1; AND SECTION XII MAXIMUM ALLOWABLE STRESS VALUES S FOR FERROUS MATERIALS

Line No.	Maximum Allowable Stress, MPa (Multiply by 1000 to Obtain kPa), for Metal Temperature, °C, Not Exceeding																
	500	525	550	575	600	625	650	675	700	725	750	775	800	825	850	875	900
1	73.6	72.4	70.8	68.9	65.4	51.4	41.7	32.9	26.5	21.3	17.2	13.9	11.1	8.73
2	99.3	98.0	93.3	79.6	65.4	51.4	41.7	32.9	26.5	21.3	17.2	13.9	11.1	8.73
3	84.0	83.2	79.0	67.3	55.4	44.1	35.5	28.0	22.2	18.2	15.0	12.3	9.83	7.33
4	62.6	61.3	60.1	58.6	55.4	44.1	35.5	28.0	22.2	18.2	15.0	12.3	9.83	7.33
5	73.6	72.4	70.8	68.9	65.4	51.4	41.7	32.9	26.5	21.3	17.2	13.9	11.1	8.73
6	99.3	98.0	93.3	79.6	65.4	51.4	41.7	32.9	26.5	21.3	17.2	13.9	11.1	8.73
7	84.0	83.2	79.0	67.3	55.4	44.1	35.5	28.0	22.2	18.2	15.0	12.3	9.83	7.33
8	62.6	61.3	60.1	58.6	55.4	44.1	35.5	28.0	22.2	18.2	15.0	12.3	9.83	7.33
9	99.3	98.0	93.3	79.6	65.4	51.4	41.7	32.9	26.5	21.3	17.2	13.9	11.1	8.73
10	73.6	72.4	70.8	68.9	65.4	51.4	41.7	32.9	26.5	21.3	17.2	13.9	11.1	8.73
11	84.0	83.2	79.0	67.3	55.4	44.1	35.5	28.0	22.2	18.2	15.0	12.3	9.83	7.33
12	62.6	61.3	60.1	58.6	55.4	44.1	35.5	28.0	22.2	18.2	15.0	12.3	9.83	7.33
13	99.3	98.0	93.3	79.6	65.4	51.4	41.7	32.9	26.5	21.3	17.2	13.9	11.1	8.73
14	73.6	72.4	70.8	68.9	65.4	51.4	41.7	32.9	26.5	21.3	17.2	13.9	11.1	8.73
15	84.0	83.2	79.0	67.3	55.4	44.1	35.5	28.0	22.2	18.2	15.0	12.3	9.83	7.33
16	62.6	61.3	60.1	58.6	55.4	44.1	35.5	28.0	22.2	18.2	15.0	12.3	9.83	7.33
17
18
19
20	99.3	98.0	93.3	79.6	65.4	51.4	41.7	32.9	26.5	21.3	17.2	13.9	11.1	8.73
21	73.6	72.4	70.8	68.9	65.4	51.4	41.7	32.9	26.5	21.3	17.2	13.9	11.1	8.73
22	99.3	98.0	93.3	79.6	65.4	51.4	41.7	32.9	26.5	21.3	17.2	13.9	11.1	8.73
23	73.6	72.4	70.8	68.9	65.4	51.4	41.7	32.9	26.5	21.3	17.2	13.9	11.1	8.73
24	99.3	98.0	93.3	79.6	65.4	51.4	41.7	32.9	26.5	21.3	17.2	13.9	11.1	8.73
25	99.3	98.0	93.3	79.6	65.4	51.4	41.7	32.9	26.5	21.3	17.2	13.9	11.1	8.73
26
27
28
29	99.3	98.0	93.3	79.6	65.4	51.4	41.7	32.9	26.5	21.3	17.2	13.9	11.1	8.73
30	73.6	72.4	70.8	68.9	65.4	51.4	41.7	32.9	26.5	21.3	17.2	13.9	11.1	8.73
31	99.3	98.0	93.3	79.6	65.4	51.4	41.7	32.9	26.5	21.3	17.2	13.9	11.1	8.73
32	73.6	72.4	70.8	68.9	65.4	51.4	41.7	32.9	26.5	21.3	17.2	13.9	11.1	8.73
33
34	84.0	83.2	79.0	67.3	55.4	44.1	35.5	28.0	22.2	18.2	15.0	12.3	9.83	7.33
35	62.6	61.3	60.1	58.6	55.4	44.1	35.5	28.0	22.2	18.2	15.0	12.3	9.83	7.33
36
37
38
39

تقليل تكون السخام المتكون نتيجة إحتراق الوقود بواسطة إستخدام بعض المضيفات الاكسوجينية

إعداد

خليفة عيسى محمد بورشيد

المشرف

الأستاذ الدكتور محمد احمد حمدان

ملخص

تم دراسة عملية تقليل السخام في الوقود وذلك عن طريق استخدام بعض المضيفات الأكسوجينية بواسطة استخدام الأنبوب الحراري . وذلك لاستخدامه في التطبيقات الصناعية التي يستخدم الوقود بكثرة لتقليل التلوث الناتج عنه . تميزت هذه الطريقة بإعطاء أداء ثابت للوقود بالإضافة للمحافظة على خصائصه وإنتاج كمية أقل من السخام مقارنة مع الوقود غير المحسن بالمضيفات الأكسوجينية.

أظهرت النتائج بواسطة مقارنة نتائج تجارب مختلفة قبل وبعد إضافة المضيفات الأكسوجينية لمعرفة تأثيرها مع الوقود تقاربا ملحوظا بين كل النتائج التجريبية السابقة . حيث كان للمضيفات الأكسوجينية دور كبير في تقليل نسبة السخام.